Quantum Electronics **48** (11) 1062–1066 (2018)

LASER APPLICATIONS AND OTHER TOPICS IN QUANTUM ELECTRONICS https://doi.org/10.1070/QEL16610

Enhancing the signal-to-noise ratio for laser ranging by adjusting the photon equivalent threshold of a multi-pixel photon counter

G. Zhang, X. Yan

Abstract. **A photon equivalent (PE) threshold-adjusting regime for laser ranging is proposed based on a multi-pixel photon counter (MPPC), and the mechanism of PE threshold influence on the signal-to-noise ratio (SNR) is demonstrated and analysed. The unique PE threshold adjustability of an MPPC leads to interesting results for laser ranging. Experimental results show that the SNR of the laser ranging system is significantly improved by optimising the MPPC PE threshold, which is beneficial for detection and false alarm probabilities. Submillimeter laser ranging resolution is obtained with noncooperative targets placed several meters away. Nanosecond dead time single photon laser ranging without gating is obtained due to an MPPC with a small pixel area. Multiple target ranging is implemented with a single MPPC rather than an array.**

Keywords: *signal-to-noise ratio, multi-pixel photon counter, photon equivalent threshold.*

1. Introduction

Laser ranging is important in many applications, such as geomorphology, reconnaissance, sports, and the military science [1–3]. Time-of-flight laser pulses are widely used to measure distances directly [1–4]. Higher-ranging capability has been obtained using superconducting single-photon detectors (SPDs) and avalanche photodiodes (APDs) as laser ranging detectors [5–8]. For these purposes, superconducting SPDs have to operate at cryogenic temperatures, necessitating relatively complex and bulky setups [5, 6], thus limiting their practical application in laser ranging. APDs, however, can be operated in two regimes, linear and Geiger modes. When APDs operate in linear mode, they have a limited gain (usually no greater than 1000), which makes it difficult to detect single photon-level echo signals. The sensitivity of laser ranging receivers has been improved using a Geiger-mode APD (Gm-APD, also called a single photon avalanche photodiode, SPAD) as a detector of their ranging systems because of their extremely high sensitivity [7–10]. However, SPADs have a few drawbacks, including that these devices are a kind of a binary photon counting device without photon number resolving (PNR) capability; a SPAD can judge whether there are photons or not, but it cannot count the number of photons in the echoed light signal [11]. Moreover, the intensity of the pulsed light signal reflected from the target, which might be significant in laser radar imaging, cannot be accurately reconstructed. Another drawback of a SPAD is that it experiences a 'dead time' during which it cannot function after a photon is detected [3], an effect that might distort the true arrival time of echoed signal photons. Thus, using a SPAD with a shorter 'dead time' is necessary. Unfortunately, a shorter 'dead time' is a tradeoff in light sensitivity, after-pulsing probability, and photon detection efficiency, which limits the minimum available SPAD 'dead time'. In addition, to quickly quench an avalanching SPAD and to minimise the influence of large dark counts and after-pulsing effects, SPADs have to be operated in a gated-Geiger mode, involving a DC reverse bias applied to the APD and combined with a short electric gating pulse [12, 13]. In this operating regime, such a SPAD is not suitable for ranging a target at an unknown distance [8], because one has to scan the detecting gate to synchronise with photons reflected from the target, which thus slows the ranging speed. It would be best if it were feasible to range a target placed at an unknown distance without gating.

To overcome the above-mentioned problems, a few research groups have employed a new kind of a photon counter that is currently under development, i.e., multi-pixel photon counter (MPPC) as a detector for laser ranging [11, 14]. Range resolutions on the order of 10 cm with targets from tens to hundreds of meters away have been obtained and the 'dead time' of these MPPCs is ~100 ns. However, the factors influencing the system signal-to-noise ratio (SNR) have not been addressed, which determines the detection and false alarm probabilities of a laser ranging or lidar system.

In this paper, a photon equivalent (PE) threshold-adjusting scheme for laser ranging is proposed and the influence of the PE threshold (Th) on the SNR is demonstrated and analysed. The results show that the SNR of a laser ranging system are noticeably increased by optimising the Th of MPPCs.

2. PE-threshold adjusting scheme for laser ranging

An MPPC is a kind of a spatial multiplexing photon that can proportionally output distinguishable avalanche pulses (proportional to the number of photons) when the photon flux is within the linear response region of the MPPC, which is different from other avalanche based detectors. In its linear responding region, the MPPC is a quasi-ideal photon detector, with detected photons in a certain time approximately described by the famous Poisson distribution. This is valid if the intensity of the reflected light from the target is steady in a certain time and the M factor (product of the space

G. Zhang, X. Yan School of Science, Xi'an Polytechnic University, Xi'an, 710048, China; e-mail: zhangg_365@163.com

Received 9 January 2018
Kvantovaya Elektronika **48** (11) 1062–1066 (2018)
Submitted in English

model number of the receiving light field and time bandwidth) is much larger than unity [15], which is the common case for laser ranging. For a real detector, the Poisson distribution also describes well the dark counts [9, 16]. Thus, the occurrence probability of a k photon equivalent pulse from an MPPC in a certain time is expressed as

$$p_{\mathrm{ps}}(k) = \frac{[(s+b)\eta + K_{\mathrm{d}}]^k \exp[-(s+b)\eta - K_{\mathrm{d}}]}{k!}, \tag{1}$$

where $k = 0, 1, 2, 3, \ldots$; $p_{\mathrm{ps}}(k)$ is the probability of k 'detected photons', or more exactly an event (denoted as a k PE event), which has proved applicable for the MPPC in many studies [15, 17, 18]; s and b are the mean number of echo signal and background photons, respectively; η is the photon detection efficiency; and K_{d} are the dark counts. Similarly, the occurrence probability of a k PE pulse from the MPPC without an echo signal photon is

$$p_{\mathrm{ps}}(k) = \frac{(b\eta + K_{\mathrm{d}})^k \exp[-(b\eta - K_{\mathrm{d}})]}{k!}. \tag{2}$$

Considering a ranging measurement with N (a large number) laser pulse events, the expectant event counts, in which the amplitude of the PE output from the MPPC was larger than the Th value of a discriminator, which included both echo and background photons as well as dark counts and denoted as $N_{\text{with echo}}$, was expressed as

$$\begin{aligned} N_{\text{with echo}} &= N \sum_{k=\mathrm{Th}}^{\infty} p_{\mathrm{ps}}(k) \\ &= N \sum_{k=\mathrm{Th}}^{\infty} \frac{[(s+b)\eta + K_{\mathrm{d}}]^k \exp[-(s+b)\eta - K_{\mathrm{d}}]}{k!}. \end{aligned} \tag{3}$$

Similarly, the expectant event counts with the amplitude of the output pulse without echo signal photons, larger than Th, was

$$N_{\text{no echo}} = N \sum_{k=\mathrm{Th}}^{\infty} \frac{(b\eta + K_{\mathrm{d}})^k \exp[-(b\eta + K_{\mathrm{d}})]}{k!}. \tag{4}$$

The Th value was often set to 0.5, 1.5, and 2.5 PE, etc., to avoid misjudging the detected photon number and thus eliminate the influence of electrical noise. Then, the SNR was obtained by substituting Eqns (3) and (4) into

$$\mathrm{SNR} = \frac{N_{\text{with echo}} - N_{\text{no echo}}}{\sqrt{N_{\text{with echo}} + N_{\text{no echo}}}}. \tag{5}$$

It was natural to expect that, by changing the Th, the SNR would be accordingly changed. As matter of fact, as the background photons and dark counts of a detector are usually randomly distributed in time and the echoed photons are much more concentrated, the average nonecho counts ($N_{\text{no echo}}$) in a time bin should be much smaller than the total counts with echoed photons. Thus, most of the $N_{\text{no echo}}$ might be eliminated by increasing the Th to a few PE and, as a result, the SNR would be increased. In this case, of course, some of the echoed photons were sacrificed, but many more background and dark counts were eliminated, which will be proved in Section 4. In practice, one can just count the counts in each time bin to obtain $N_{\text{with echo}}$ and $N_{\text{no echo}}$ without using Eqns (3) and (4).

3. Experimental setup and method

The above idea was verified, and the properties of the proposed regime were demonstrated, using a laser ranging system that included an MPPC and integrated time correlated single photon counting (TCSPC) card (SPC-150, time resolution capability 813 fs per time channel, 10 MHz saturated count rate, Becker & Hickl GmbH, Berlin, Germany). The schematic of the setup is shown in Fig. 1. The MPPC [C11209-110, photosensitive area 1×1 mm, 10×10 μm^2 each pixel, 10^4 pixels, dark count rate (DCR)/100 kHz at 25 °C at the recommended bias voltage, Hamamatsu Photonics K. K., Hamamatsu City, Japan] was fired by echoed photons from a picosecond laser source (centre wavelength, 670 nm; full width at half maximum, 44 ps; repetition rate, 31.125 kHz–80 MHz; maximum average light power, 0.7 mW; PDL-800D, PicoQuant, Berlin, Germany), and the laser pulse was expanded by a beam expander. The diffusely reflected light from noncooperative targets was collected by a lens group and coupled to the MPPC. Moreover, a narrow band-pass filter (centre wavelength, 670 nm; bandpass width, 16 nm; and OD, 4) was fixed in front of the MPPC to block most background photons. Also, the response avalanche signals from the MPPC were first amplified by a fast amplifier (3 dB band width; 10 kHz–

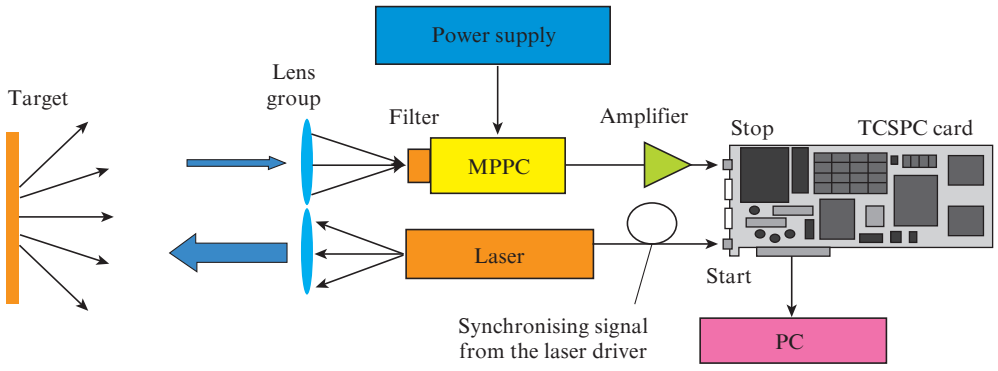

Figure 1. Schematic of the laser ranging setup with MPPC and an integrated TCSPC card. The value of Th is adjusted by the built-in constant fraction discriminator (CFD) of the TCSPC card.

1.9 GHz; noise figure, 4.9 dB; fixed voltage gain, 40 dB, 100×; HSA-Y-2-40, Femto, Inc., Chelmsford MA, USA). The signal was then placed in the stop channel of the TCSPC card, which possessed a built-in constant fraction discriminator (CFD) that facilitated adjustment of the Th value for optimising the SNR for laser ranging. Meanwhile, the synchronising signal from the laser driver was placed in the TCSPC card start channel. Next, the TCSPC card began to record the time stamp and time interval once the start channel accepted a signal pulse, until the stop channel received an effective pulse from the MPPC. The TCSPC card recorded tens of thousands of time intervals between pulses from the two channels, after which the card transmitted a statistical histogram data of these time intervals to a PC. Then, the histogram distribution curve of the time intervals was obtained, with a clear peak in distribution if the MPPC received echo light from the targets, which defined the arriving time of echoed photons. By changing the Th of the CFD, multiple time distribution histograms were obtained in several measurements.

The distance between a reference target and target was obtained with the following TOF (time-of-flight) equation

$$D = \frac{1}{2}c\Delta t = \frac{1}{2}c(t_t - t_{ref}), \tag{6}$$

where c is the speed of light in the atmosphere; and t_t and t_{ref} are the time position of the 'target peak' and 'reference target peak' of the histograms, respectively.

In addition, a digital phosphor oscilloscope was used (DPO4102B-L, 5 GSa/s, 1 GHz bandwidth, Tektronix Inc., Beaverton, OR, USA) to ascertain the Th amplitude and observe the waveforms. The range measurement accuracy of the system was checked using a portable commercial laser range finder (SW-M-100, Sndway Inc., Guangdong, China).

4. Results and analysis

4.1. Waveform analysis and determination of the Th amplitude

Oscillograms with a synchronising signal or start signal and a single photon responding avalanche signal or stop signal from an MPPC clearly showed the multiple avalanche pulses (1, 2, 3 PE, etc.), which indicated good PNR capability by the MPPC. Because of this capability, the CFD Th was easily adjusted to optimise the SNR of the laser ranging system if the background photon flux was relatively high, which will be discussed in Section 4.2. This Th adjustability was unique for MPPCs and not applicable for other APD-based detectors. In Fig. 2, the horizontal line between 1 and 2 PE indicates the position of the 1.5 Th threshold. In addition, the 1 PE avalanche pulse was observed to have a rise time of ~500 ps and the fall time, which determined the dead time, was ~5 ns. Such a short dead time, which was even smaller than for most of commercial, active-quenching SPADs [19,20], was attributed to the small pixel area and thus small pixel capacitance of the MPPC, which was beneficial for minimising photon-counting loss and enhancing range resolution between two close targets.

4.2. Multiple target ranging results and Th influence on the ranging SNR

The histogram distribution curves for the time intervals between start and stop pulses acquired by the TCSPC card at midday of a sunny day showed that the background illuminance in the laboratory was about 1000 lux, while the background counts were observed to be very small (Fig. 3). This was because the Th value was adjusted to 3.5 PE, which eliminated most of the background and dark counts. The solid curve is the time interval distribution of the output pulses from the MPPC, pulses were triggered by photons reflected from a reference target (a small noncooperative plastic plate) or by background photons or dark carriers from the MPPC itself. The dashed curve which shows the distribution of time intervals of the avalanche pulses from the MPPC, was triggered by echoed photons from target 1 (wall). The distance between target 1 and the reference target was then calculated by Eqn (6) using the time difference between the two peaks in Fig. 3, which is shown below.

Three important observations were obtained from analysis of the three peaks in a three-target time distribution with different Th values; target 1 was the farthest and target 3 was

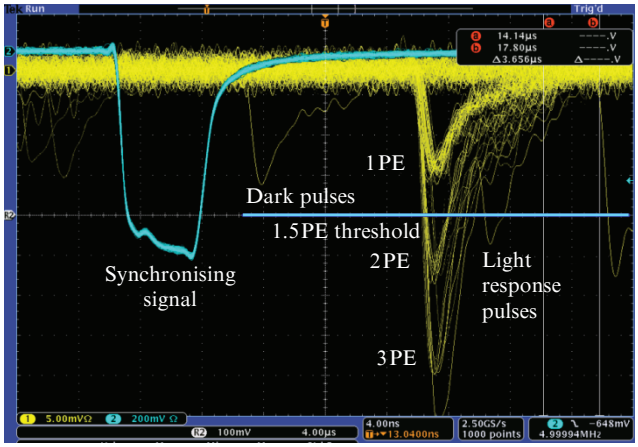

Figure 2. Oscilloscope screenshot with a synchronising signal or a 'start' signal and single photon responding avalanche signal or 'stop' signal from an MPPC.

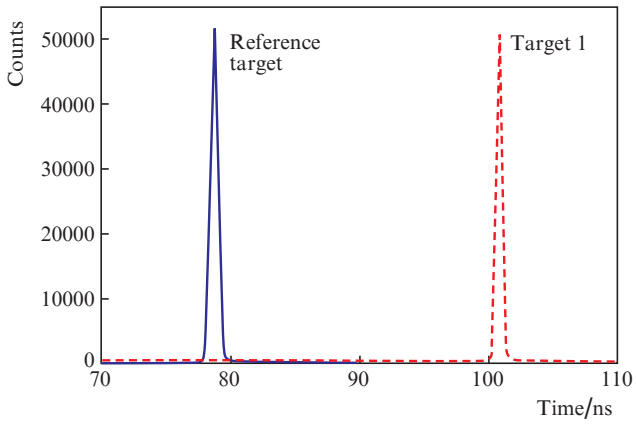

Figure 3. Histograms of the time intervals between start and stop pulses acquired by the TCSPC card. The acquisition time was 60 s and the laser pulse repetition rate was 1 MHz, with the average laser power adjusted to avoid saturating the MPPC.

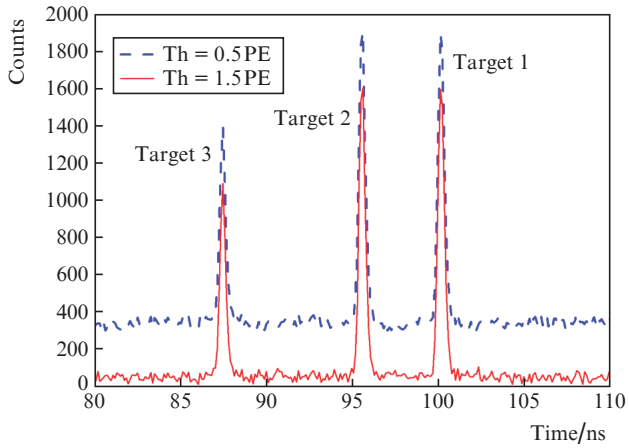

Figure 4. Time distribution of echo photons from three targets with different Th. Target 1 is the laboratory wall; targets 2 and 3 are two small white boards which partly blocked laser light paths; the data acquisition time is 2 s.

the nearest (Fig. 4). The first observations was that the SNR was enhanced by adjusting the Th, as it was evident that background counts were much smaller with Th = 1.5 PE than with Th = 0.5 PE. With the observed peak counts and average background counts shown in Fig. 3, the SNR was calculated using Eqn (5). With target 2, as an example, the SNR was 32 if Th was 0.5 PE. In contrast, it approached ~38.2 when the Th was 1.5 PE, although some of the useful echoed photons were sacrificed. In practice, the optimised Th should be a tradeoff to eliminate background counts (false alarm counts) as well as avoid too many lost echoed signal photons. These results indicated a means for optimising the detection and false alarm probabilities, which are key parameters for laser ranging and lidar.

The second observation was that submillimeter ranging accuracy was obtained. If the time position of the maximum value of each peak was considered as the 'true' arriving time of echoed photons from targets, the distances between these targets and the reference target were calculated according to the data of this figure and Eqn (6), which were 3318.3, 2641.1, and 1420.0 mm for targets 1, 2, and 3, respectively. As the time resolution per channel of this TCSPC card was 813 fs [21], which corresponded to a 0.24 mm error value, submillimeter ranging accuracy was expected. In order to check the range measurement accuracy of the system, the results should be compared with a more precise laser range finder. However the available laser range finder we have can only obtain ±0.5 mm accuracy. The distance value of these targets obtained by this laser range finder was 3318±0.5, 2641±0.5, and 1419±0.5 mm, respectively, which was in good agreement with the value measured by the present system.

The third observation was that multiple target distances were obtained with a single MPPC, rather than using a detector array [10].

It was noteworthy that, during the whole measurement process, no gating was used to eliminate background photons or to increase the SNR, which is important in laser ranging if the approximate distance to a target is unknown. This was due to the situation that, if one APD pixel of an MPPC was fired (triggered) by a photon or a dark carrier and had not recovered yet, the other APD pixels were still ready to respond to incoming photons, which reduced the effective dead time and relieved the unfavourable effects of background photons and dark counts as well as after-pulses. In addition, the PNR capability of an MPPC made it easy to obtain echo intensity information and target distance information at the same time, which are both useful for laser radar imaging.

5. Conclusions

The Th adjusting regime for laser ranging based on an MPPC was proposed and the mechanism for the influence of the Th value on the SNR was demonstrated and analysed. The SNR was significantly improved by optimising the MPPC's Th, which was beneficial for the detection and false alarm probabilities. Multiple target distances were obtained with a single MPPC. A submillimeter laser ranging resolution was obtained with noncooperative targets several meters away. Nanosecond level dead time and single photon laser ranging without gating was obtained using an MPPC with a small pixel area.

Acknowledgements. The work was supported by the National Natural Science Foundation of China (Nos 11405119 and 61405151) and Natural Science Basic Research Plan in Shaanxi Province of China (Grant No. 2014 JQ8364).

References

1. Blais F. *J. Electron Imaging*, **13** (1), 231 (2004).
2. Warburton R.E., McCarthy A., Wallace A.M., Hernandez-Marin S., Hadfield R.H., Nam S.W., Buller G.S. *Opt. Lett.*, **32** (15), 2266 (2007).
3. Oh M.S., Kong H.J., Kim K.H., Jo S.E., Kim B.W., Park D.J. *J. Opt. Soc. Am. A*, **28**, 759 (2011).
4. McCarthy A., Collins R.J., Krichel N.J., Fernández V., Wallace A.M., Buller G.S. *Appl. Opt.*, **48** (32), 6241 (2009).
5. Warburton R.E., McCarthy A., Wallace A.M., Hernandez-Marin S., Hadfield R.H., Nam S.W., Buller G.S. *Opt. Lett.*, **32** (15), 2266 (2007).
6. Lobanov Y., Shcherbatenko M., Semenov A., Kovalyuk V., Kahl O., Ferrari S., Korneev A., Ozhegov R., Kaurova N., Voronov B.M., Pernice W.H.P., Gol'tsman G.N. *IEEE Trans. Appl. Supercondict.*, **27** (4), 2200705 (2017).
7. Albota M.A., Heinrichs R.M., Kocher D.G., Fouche D.G., Player B.E., O'Brien M.E., Aull B.F., Zayhowski J.J., Mooney J., Willard B.C., Carlson R.R. *Appl. Opt.*, **41** (36), 7671 (2002).
8. Oh M.S., Kong H.J., Kim T.H., Kim K.H., Kim B.W., Park D.J. *Rev. Sci. Instrum.*, **81**, 033109 (2010).
9. Ren M., Gu X.R., Liang Y., Kong W.B., Wu E., Wu G., Zeng H.P. *Opt. Express*, **19**, 13497 (2011).
10. Gatt P., Johnson S., Nichols T. *Appl. Opt.*, **48** (17), 3261 (2009).
11. Kyu Tak Son, Chin C. Lee. *IEEE Trans. Instrum. Measurement*, **59** (11), 3005 (2010).
12. Zhang J., Thew R., Barreiro C., Zbinden H. *Appl. Phys. Lett.*, **95** (9), 091103 (2009).
13. Zhang J., Eraerds P., Walenta N., Barreiro C., Thew R., Zbinden H. arXiv: 1002.3240v1 [quant-ph], (2010).
14. Adamo G., Busacca A. *AEIT Internat. Annual Conf.* (Capri, Naples, 2016).
15. Goodman J.W. *Statistical Optics* (New York: Wiley, 1985).
16. Renker D., Lorenz E. *J. Instrument.*, **4**, 1 (2009).
17. http://www.hamamatsu.com/us/en/community/optical_sensors/articles/measuring_characteristics_of_mppc/index.html, Accessed 19 June, 2017.

18. Acerbi F., Ferri A., Zappala G., Paternoster G., Picciotto A., Gola A., Zorzi N., Piemonte C. *IEEE Trans. Nucl. Sci*., **62** (3), 1318 (2015).
19. http://www.idquantique.com/photon-counting/photon-counting-modules/id100/, Accessed 19 June, 2017.
20. Ren M., Wu G., Wu E., Zeng H.P. *Laser Phys*., **21** (4), 755 (2011).
21. http://www.becker-hickl.com/spc150.htm, Accessed 25 June, 2017.